

Ideal glass in attractive systems with different potentials

K Dawson¹, G Foffi¹, G D McCullagh¹, F Sciortino², P Tartaglia² and E Zaccarelli²

¹ Irish Centre for Colloid Science and Biomaterials, University College Dublin, Belfield, Dublin 4, Republic of Ireland

² Dipartimento di Fisica, Istituto Nazionale per la Fisica della Materia and INFN Center for Statistical Mechanics and Complexity, Università di Roma La Sapienza, Ple A Moro 2, I-00185 Roma, Italy

Received 22 November 2001

Published 22 February 2002

Online at stacks.iop.org/JPhysCM/14/2223

Abstract

We discuss the ideal glass transition for two types of potential model of attractive colloidal systems, i.e. the square-well system and the Yukawa hard-sphere fluid. We use the framework of the ideal mode-coupling theory and we mostly focus our attention on the nature of the singularities predicted by the theory. We also study the phenomena that arise by varying the range of the attraction, since this parameter has been identified as one of the key parameters in colloidal systems.

1. Introduction

One of the oldest and best studied problems in statistical mechanics involves the study of the phase diagram of simple spherical molecules with a hard-core repulsion, and a short-ranged attraction. Some of the earliest theories, such as that of van der Waals, already incorporated sufficient of the essential features of competition between attractive forces and entropy to exhibit a liquid–gas transition. Though the details are not correct, there has not been cause to significantly revise the basic picture of the phenomena in modern times. On the other hand, such theories did not well represent the contribution of the hard core, and it was much later that crystallization and imperfectly packed solids or glasses were incorporated into the story. A great importance in this area has been, recently, occupied by the study of colloidal systems. Indeed, these systems present some ideal properties that make them excellent candidates for the studies of aggregation and vitrification. In particular, once a potential model is taken into consideration, the theoretical tools of statistical mechanics, for molecular liquids, can be *de facto* exported in this arena. From an experimental point of view, the larger dimensions of colloidal particles, with respect to simple molecules, allow us to study them more easily.

The study of the glass transition in colloidal systems has been one of the most striking cases of verification of the current theories of super-cooled liquids. The systems used experimentally [1, 2], colloidal particles in solution, are very closely represented by hard

spheres, where only excluded volume effects are important at high concentration. Moreover, in contrast to molecular liquids, it is much easier to avoid the crystalline phase and produce a colloidal glass. From the theoretical point of view hard spheres are the simplest systems where analytical theories can be relatively easily exploited. We refer in particular to the mode-coupling theory (MCT) of super-cooled liquids [3], which in recent years has been more and more widely used in diverse systems to interpret experimental data rather successfully [4]. The agreement between MCT and experiments is quite satisfactory and the details of the time correlation functions are well reproduced. In particular, on approaching the liquid–glass threshold in concentration, hard-sphere systems show a non-ergodic transition. It is widely believed that in super-cooled molecular liquids a real non-ergodicity transition is avoided by the onset of different dynamical mechanisms, such as hopping, which apparently do not manifest in colloids. Small discrepancies appear in the comparison between experiments and theory, the most important of which is the value of the volume fraction at the transition. In general the description of the phenomena related to the glass transition is quantitatively correct to within a few per cent.

Experiments on more complex colloidal systems show a pattern similar to the one we describe, but in some cases differences become important and cannot be easily explained in terms of the MCT applied to repulsive potentials. For example in some case the value of the non-ergodicity factor, i.e. the asymptotic value of the concentration time correlation functions in the glassy regime, attains values that are much higher than the ones predicted using only repulsive interactions [6]. Another unusual result that appears in colloids is the presence of an amorphous phase at low volume fractions [5–7], a phenomenon often called colloidal gelation. A line of thermodynamic states corresponding to structural arrest, observed through dynamic light scattering, was observed in systems tailored to have an attractive interaction. This locus in some cases intersects the binodal line and is referred to as transient gelation when observed in the spinodal region. More recently concentration time correlation functions have been observed in a polymeric system with a decay time much longer than the usual stretched exponential, i.e. a logarithmic time relaxation [8]. All these facts point in the direction of the necessity of going beyond the simple hard-sphere system and adding an attractive component in addition to the repulsive interaction.

From the theoretical point of view, interesting advances were made once attractive systems were studied within MCT. We have started the study of the influence of attractive forces in a simple model, the Baxter limit, which is the appropriate limit of an infinitely deep square well of zero width [9]. Due to the unsatisfying behaviour of this model [10, 11, 30], the attention has been moved to more realistic types of potential, such as the attractive Yukawa [12] and the square-well potential [13]. In both these approximations some new behaviour appears which shows a pronounced resemblance to what is observed in some attractive colloids. We refer in particular to the high values of the non-ergodicity factors and to the presence of liquid–glass transition points for low values of the concentration of the dispersed phase. In the case of the square-well potential instead we observed, for dense colloids, a re-entrant behaviour of the glass line, accompanied by the appearance of higher-order transition points where a logarithmic decay of the correlation functions arises [13]. These phenomena appear when the width of the square well is very short compared with the radius of the colloidal particles. Thus, the presence of attractions produces a whole new range of interesting phenomena, particularly for very narrow wells.

Indeed, it seems clear that one of the main parameters responsible for the physical behaviour of attractive colloidal suspensions is the range of the attraction. For example, computer simulations and experiments have shown that when the range of the potential is below a certain value, the typical fluid–fluid phase transition becomes metastable with respect to a

fluid–solid transition. Moreover, the presence of a real thermodynamic solid–solid coexistence line has been detected [14, 15]. It is therefore not surprising that the range of the potential also plays a key role in non-equilibrium phenomena such as glassification studied within MCT.

In this paper we review results for the SW system and present results obtained by solving an attractive Yukawa potential treated with a self-consistent approximation that has already proven to be rather accurate in describing the static correlations in a liquid. In particular the aim of the paper is to check whether the phenomena, already observed for SWS solved both within Percus–Yevick approximation (PYA) and mean spherical approximation [13], are robust enough to not crucially depend on the choice of the potential model, as well as on the approximation considered to calculate the thermodynamics of the system.

The paper is organized as follows: in section 2 we discuss both the Percus–Yevick solution for HSS and the self-consistent approach to the Yukawa fluid. In section 3 a brief review of the main feature of MCT will be proposed. Finally in section 4 the results for SWS and Yukawa will be presented and analysed.

2. Calculation of the structure factors

Since the equilibrium static structure factor is the main input of MCT in this section we shall discuss its definition and its properties. In particular we shall focus on the two fluid models we solved in order to obtain this quantity, i.e. square-well and Yukawa model.

The structure factor S_q is defined as the equal time correlation function of the density variable in wavevector space,

$$S_q = \langle \rho_{-q}(t) \rho_q(t) \rangle = \langle \rho_{-q}(0) \rho_q(0) \rangle \quad (1)$$

where the average $\langle \dots \rangle$ is performed at equilibrium and ρ_q are the density variables, i.e. $\rho_q = \sum_i e^{iq \cdot r_i}$. This quantity gives information about the structure of the system and can be measured in light scattering experiments. A fundamental relation is the Ornstein–Zernike (OZ) equation, which relates the total correlation function, $h(r) = g(r) - 1$, to the direct correlation function $c(r)$,

$$h(r) = c(r) + \rho \int dr' c(|\mathbf{r} - \mathbf{r}'|) h(r'). \quad (2)$$

The Fourier transform of the direct correlation function c_q is, thus, related to the static structure factor S_q by

$$S_q = \frac{1}{1 - \rho c_q}. \quad (3)$$

In the following subsections we shall describe the procedures adopted to solve the OZ equation for the SW model and for the HYF.

2.1. Percus–Yevick SW

The SW model is defined by the potential,

$$v(r) = \begin{cases} \infty & 0 \leq r \leq d \\ -u_0 & d \leq r \leq d + \Delta \\ 0 & r > d + \Delta \end{cases} \quad (4)$$

where d is the diameter of the colloidal particles. In this paper the quantity u_0 has been set to unity. We also define the well width parameter $\epsilon = \Delta / (d + \Delta)$. The system is then specified once we have specified the temperature T (we shall work in units of k_B), the packing fraction $\phi = \pi d^3 \rho / 6$ and the well-width parameter ϵ . In order to obtain the static structure factor

for the SW model we have used the so-called Weiner–Hopf factorization of the OZ equation introduced by Baxter [22]. Considering the auxiliary function $Q(r)$ which satisfies the set of equations

$$\begin{aligned}rc(r) &= -Q'(r) + 2\pi\rho \int_r^{R'} dt Q'(t)Q(t-r) & 0 < r < R' \\rh(r) &= -Q'(r) + 2\pi\rho \int_0^{R'} dt (r-t)h(|r-t|)Q(t) & r > 0\end{aligned}\quad (5)$$

where $Q'(r)$ is the derivative of $Q(r)$, it is possible to show that equation (5) is another formulation of the OZ relation (2) and that for the static structure factor we have [19]

$$S(q)^{-1} = \tilde{Q}(q)\tilde{Q}(-q) \quad (6)$$

where the Fourier transform of $Q(r)$ is given by

$$\tilde{Q}(k) = 1 - 2\pi\rho \int_0^{R'} dr e^{ikr} Q(r). \quad (7)$$

This factorization scheme has been proven to work for models where $c(r) = 0$ beyond a certain distance $r > R'$. It is clear that, as for the OZ relations (2), (5) are not closed. In order to close them we have adopted the PYA for the $c(r)$, which is expressed by the relation

$$c(r) = g(r)[1 - \exp(V(r)/k_B T)]. \quad (8)$$

Once we insert (8) into the first of equations (5) we obtain

$$e^{-u_0/k_B T} G(r) = ar + b - 2\pi\rho \int_r^{d+\Delta} ds Q'(s)Q(s-r) + 2\pi\rho \int_0^{r-d} ds G(r-s)Q(s) \quad (9)$$

where the terms a and b are obtained from the solution for the hard-sphere system (HSS) and $G(r) = rg(r)$. Equation (9) has been solved numerically on an equally spaced grid of points r_n with $n = 1, 2, \dots, 1000$. Both $G(r)$ and $Q(r)$ have been evaluated by numerical iteration. The function $Q(r)$ was integrated numerically from $Q'(r)$ with a five-point formula. The results were accepted once the absolute differences in the solution, for two successive iterations, had reached the value 10^{-12} . The method here discussed seems to work properly for values of the well-width parameter up to 0.1, after which the algorithm becomes unstable.

2.2. Scoza

In this section we shall describe the self-consistent Ornstein–Zernike approximation (SCOZA) [16, 17] that we have used to calculate the structure factors of the hard-core Yukawa fluid. The interaction potential is expressed by

$$v(r) = \begin{cases} \infty & 0 \leq r \leq d \\ e^{-b(r-d)} & r \geq d \\ -\epsilon \frac{r-d}{r/d} & r \geq d \end{cases} \quad (10)$$

where, again, d is the diameter of the particles. The parameter b , known as the screening parameter, modulates the range of the potential, i.e. the larger b the shorter the range of the potential. This potential can be chosen as a proper representation of the interaction potential of many colloidal systems, and, for values of b between 2 and 9, it corresponds roughly to a Lennard–Jones potential, which represents a more realistic choice for atomic and molecular systems. However, for many colloidal [6] and protein [18] systems interacting with a short-range potential, the Yukawa potential with a large value of b can represent an interesting choice. The idea behind SCOZA is to provide a closure relation for $c(r)$, in terms of $\beta v(r)$,

that depends on one or more state-dependent parameters that can be adjusted in order to get the thermodynamics of the system correctly. It is well known, indeed, that one of the main problems in the classical integral equations is the lack of consistency between different routes to calculate the various thermodynamical properties [19]. Self-consistent theories overcome such a problem by building the consistency within the theory itself. The SCOZA approach we adopted is based on only one parameter K , i.e.

$$c(r) = -K\beta v(r) + B e^{-\lambda(r-\sigma)}/r. \quad (11)$$

The Yukawa term in equation (11) is added to take into account the hard-sphere contribution outside the core, whereas inside it we have, for obvious reasons, $g(r) = 0$. The parameters B and λ are evaluated by setting $V(r) = 0$ in equation (11) and requiring that compressibility and the virial equation of state give the same answer, which is chosen to be the Carnahan–Sterling (CS) solution for hard spheres [19, 20]. Thermodynamical consistency is then imposed by requiring that the compressibility and the energy state equations yield the same results. It can be shown that this is equivalent to the thermodynamical condition [16]:

$$\frac{\partial}{\partial \beta} \left(\frac{1}{\chi_{\text{red}}} \right) = \rho \frac{\partial^2 u}{\partial \rho^2} \quad (12)$$

where χ_{red} is the reduced compressibility, obtained by the compressibility sum rule of S_q for $q = 0$, while u is the energy obtained by the integral of the attractive tail over the radial distribution function $g(r)$. If we substitute (11) into (12) a PDE is obtained for the function $K(\rho, \beta)$. In the case of the Yukawa interaction there is an analytical relation for the compressibility that allows us to obtain a solution for u [17, 21] and consequently to easily determine $K(\rho, \beta)$.

The two main benefits in using SCOZA are respectively the thermodynamical consistency built into the theory itself, which makes it a more favourable choice than the standard integral equations (PY, MSA, HNC etc [19]), as well as the good agreement between SCOZA results and numerical simulations. In particular for b up to 9 the results for spinodal and binodal lines seem to agree quite well with results of SCOZA [16].

To conclude this section, that does not pretend by any means to be exhaustive, we stress that once the direct correlation is obtained by equation (11) it is possible to Fourier transform it easily in order to get the static structure factor S_q , which is the input we used to solve the MCT equations.

3. Mode-coupling theory and the glass transition

MCT provides a set of equations that allow us to calculate the dynamical density–density correlation function from the only static inputs of static structure factor, S_q , and number density, $\rho = N/V$. Here we shall focus only on the static limit of the theory, which allows us to determine the location of the ideal liquid–glass transition. In what follows we shall follow the original derivation [3] but, recently, a new approach based on a stochastic idea has been proposed leading to the same results [23]. The normalized correlators are defined as

$$\Phi_q(t) = \frac{\langle \rho_q^*(t) \rho_q \rangle}{\langle |\rho_q|^2 \rangle} = \frac{S_q(t)}{S_q}. \quad (13)$$

These quantities, and their Fourier transform in time, can be tested versus experiments using dynamic light scattering (DLS) or neutron scattering. We now define the long-time limit of (13), $f_q = \phi_q(t \rightarrow \infty)$. f_q is the so-called non-ergodicity parameter or Debye–Waller factor. If the system is in a fluid state, a density fluctuation created at time $t = 0$ will have disappeared

for $t \rightarrow \infty$, i.e. the system loses the memory of its initial conditions. In this situation the system is in an ergodic state, characterized by $f_q = 0$ for every q . In contrast, a glassy state is characterized by a spontaneous arrest of the density fluctuations. In such a case the system is non-ergodic, i.e. the timescale to lose memory of the initial states diverges and the system never reaches equilibrium. Thus $f_q \neq 0$ and the system is frozen in a glassy state. The transition between the two states is the ideal liquid–glass transition. When it is reached the Debye–Waller factor discontinuously becomes non-negative and equal to the critical value $f_q^c > 0$ [3].

The Debye–Waller factor obeys the algebraic set of equations [24],

$$\frac{f_q}{1 - f_q} = \mathcal{F}_q(f) \quad (14)$$

which is obtained as the long-time limit of the equation for $\Phi_q(t)$. The functional $\mathcal{F}_q(f)$ is the mode-coupling functional that contains the coupling between the different modes in the system, and it is given, in its discretized form, by

$$\mathcal{F}_q(f) = \sum_{kp} V_{q,kp} f_k f_p \quad (15)$$

where the sum runs over a grid of M equally spaced points and the MCT vertex functions $V_{\vec{q},\vec{k}}$ are determined by the structure factor S_q , the direct correlation function c_q and the density ρ :

$$V_{\vec{q},\vec{k}} \equiv S_q S_k S_{|\vec{q}-\vec{k}|} \rho [\vec{q} \cdot \vec{k} c_k + \vec{q} \cdot (\vec{q} - \vec{k}) c_{|\vec{q}-\vec{k}|}]^2 / q^4. \quad (16)$$

The glass transition emerges as a bifurcation of the solutions of the equations for the non-ergodicity parameter (14). In particular, it is clear that $f_q = 0$ is always a solution of equation (14). When more than a solution emerges, it is possible to show that the non-ergodicity parameter is the largest of all the solutions of the equation. This result is known as the theorem of the maximum [3]. In what follows equation (14) has been solved numerically applying the iterative scheme $f_q^{(n+1)} = \mathcal{F}_q[f_q^{(n)}] / (1 + \mathcal{F}_q[f_q^{(n)}])$, starting from the initial guess $f_q^{(0)} = S_q$.

To locate more precisely the glass transition points, it is possible to characterize them by calculating the eigenvalues of the stability matrix of equation (14). We shall now discuss this issue, since it is directly correlated to the nature of the singularities of the system. The stability matrix is defined as the $M \times M$ matrix

$$C_{qk} = \frac{\partial \mathcal{F}_q(f)}{\partial f_k} (1 - f_k)^2. \quad (17)$$

The maximum eigenvalue E of matrix C possesses the important property of being equal to unity at the glass transition. In other words, following the evolution of the largest of the eigenvalues of the matrix defined in (19), it is possible to define with great accuracy the glass transition as the locus of the parameter space where $E = E_c = 1$. Another key quantity in the calculation is the so-called exponent parameter λ defined as

$$\lambda = \sum_{qkp} \hat{e}_q^c C_{q,kp}^c e_k^c e_p^c \quad (18)$$

where the matrix $C_{q,kp}^c$

$$C_{q,kp}^c = \frac{1}{2} \frac{\partial^2 \mathcal{F}_q(f)}{\partial f_k \partial f_p} (1 - f_k)^2 (1 - f_p)^2 \quad (19)$$

and \hat{e} and e are the right and left eigenvalues of the matrix C , uniquely determined by the conditions $\hat{e}_q \geq 0$, $e_q \geq 0$, $\sum_q \hat{e}_q e_q = 1$, $\sum_q \hat{e}_q (1 - f_q) e_q^2 = 1$. The parameter λ is important for two main reasons. Firstly, it allows us to define the exponents of the power laws that regulate the asymptotic behaviour of the correlators $\phi_q(t)$ in the time domain. Secondly, it

varies in the range $0 < \lambda \leq 1$ and, when it reaches the unitary value, it defines a higher-order singular point.

Indeed, a correct classification of the singularities of equation (14) can be very helpful, because it has been shown that in the proximity of such singularities the asymptotic dynamics is totally defined. Singularities have all been classified and their mathematical characteristics are well known [25]. In particular equation (14) can present the simplest family of singularities, i.e. A_l , $l = 2, 3, \dots$. They are topologically equivalent to the bifurcation singularities of the real roots of real polynomials of degree l . The liquid–glass transition is, for example, an A_2 singularity, also known as a fold singularity. Higher-order singularities are the A_3 singularities, classified as cusp bifurcations. In both the SWS and the Yukawa fluid, the state of the system is determined by three parameters, i.e. density, temperature and range of the potential. The space of the parameters is then a tridimensional space where the A_2 folds will be a surface separating fluid and glass regions (and also as we shall see regions between two glasses) and they are characterized by $0 < \lambda < 1$. Similarly the A_3 folds will be lines that will be generated by the intersection of two folds and their exponent parameter will be equal to unity. The most complicated generic singularity in a three-parameter system is the meeting of two A_3 lines in an A_4 point in the three-dimensional parameter space.

With this we have concluded our description of the MCT ideal glass transition and we have exposed the classification of the singularities that we shall encounter in the following section, where the theory will be solved for the two models described in the sections 2.1 and 2.2.

4. Results

We shall describe now the structure of the phase diagram for the two models in the (ϕ, T) plane for different values of the potential range. It is important to stress, at this point, that the terminology ‘phase diagram’ it is not completely exact. Indeed as we have seen in the previous section, the glassy phase is not an equilibrium state. Nevertheless the analogy between an equilibrium phase diagram and a glass transition can be helpful. In this sense in the rest of the paper, we shall use the terminology phase diagram to refer to the glass lines in the thermodynamic parameter space. The glass lines were obtained from the numerical solution of MCT. In particular two routes were followed. Where the precision required was not crucial for the description of the main phenomena, we simply bracketed, at constant temperature, the critical value f_q^c narrowing the interval between a liquid and a glass solution. On the other hand, whenever a better accuracy was required (i.e. close to a higher-order singularity), we computed the largest eigenvalue looking for the condition $E = 1$.

We begin by analysing the phase diagram for SWS for different values of the well-width parameter ϵ . In figure 1 we present the glass lines for values of ϵ between 0.03 and 0.09 in the region of high densities in order to study the bifurcation of the system. For the largest of the width parameters, i.e. $\epsilon = 0.09$ the only singularity that is found is the continuous glass line, which, as we said, is an A_2 singularity. The transition line goes smoothly from low density to high temperature dividing the phase space into a glass and a liquid region. More interesting is the case of the smallest well width $\epsilon = 0.03$. Two main features emerge in this case, i.e. a re-entrant behaviour and a glass–glass singularity. The re-entrant behaviour of the glass line implies that it is possible to find a liquid for a packing fraction value larger than the predicted hard-sphere value, i.e. for $\phi > 0.516$. This phenomenon is due to the competition between the two glass driving forces, i.e. repulsion and attraction. The solution of the MCT equations, then, seems to suggest that, for certain ranges of the packing fraction, it is possible to pass from a glass to a liquid state and then again to a glass only decreasing the temperature. It is also possible to separate the glass line into two distinct branches, characterized by the transition

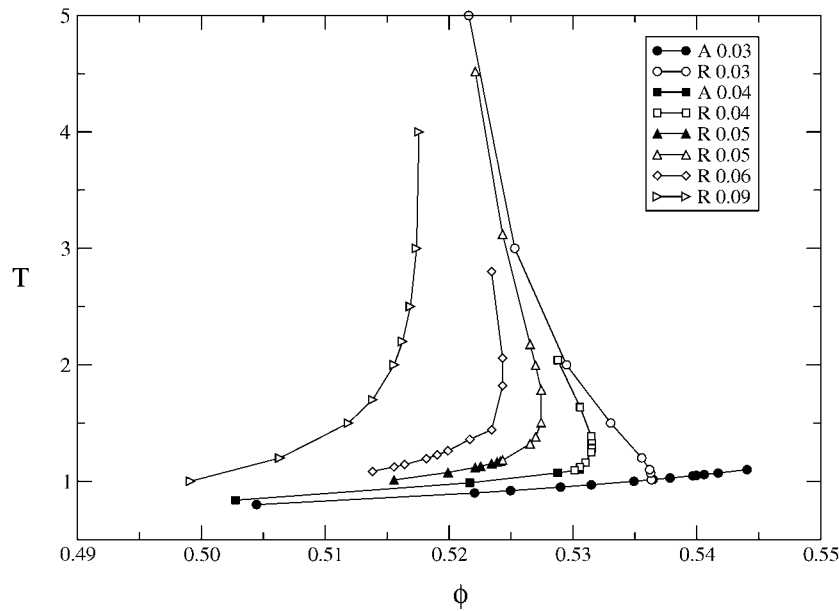


Figure 1. Phase diagram for the SWS for different values of the well-width parameter in the high-density region. For $\epsilon < 0.06$, open and full symbols represent the repulsive and the attractive glass transition respectively.

from a liquid state to an attractive and repulsive glass respectively. The two branches join at $\phi > 0.516$ with non-null angle.

The second important phenomenon is the presence, in the region of high density, of an A_2 transition line, which does not separate an ergodic from a non-ergodic state, but rather two arrested states. This has been interpreted as a transition line between two types of glass, and the higher-temperature state has been denominated repulsive glass, whereas the other one has been called attractive glass. In the former the arrest is due to repulsion and in particular to the ‘cage effect’, i.e. each particle is blocked into a cage formed by its nearest neighbours. In the latter, however, the attraction originates bonds between particles that are responsible for the arrest. In [26] the differences between these two states have been discussed studying, in particular, the rheological properties. The evolution of exponent parameter λ along the glass–glass transition curve has been also studied. We have found a cusp singularity, A_3 , that represents the endpoint of the glass–glass transition, after which the two glasses become indistinguishable and it is possible to continuously pass from a repulsive to an attractive behaviour. In figure 1 glass lines are represented also for values of $0.03 < \epsilon < 0.09$ in order to follow the evolution of the glass–glass line as a function of the well-width parameter. It can be seen that the A_3 point moves toward the liquid–glass line and consequently the transition between the two glasses tends to shrink. We have evaluated for which value of ϵ the A_3 touches the A_2 line, originating an A_4 singularity. This higher singularity has been located for $\epsilon \simeq 0.0411$. To our knowledge, this is the only model that shows this kind of full MCT singularity to date.

Up to now, we have shown results only for the high-density part of the phase diagram. Indeed another interesting feature for the systems characterized by a short-range interaction is the presence of a glassy phase up to very low densities. In figure 2 we present the phase diagram for $\epsilon = 0.03$ extended to low densities. The glass line is composed of two lines, the repulsive line, that runs almost vertically in the parameter space and the attractive line,

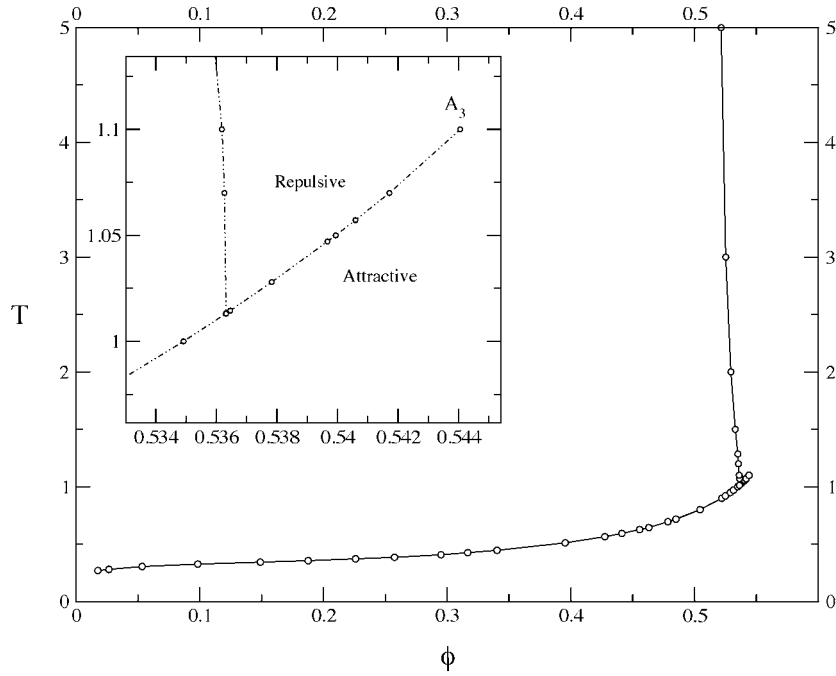


Figure 2. Glass transition line for $\epsilon = 0.03$ on a larger range of densities than in figure 1. In the inset the glass–glass transition is shown in detail.

that goes to low densities at almost constant temperature. Again the shape of these two lines is representative of the forces that originate the arrest in the two glasses. Indeed, when the repulsion is dominant, there is no energy scale and we expect the temperature to play no role; in contrast when the attraction dominates the system, we expect the transition to happen more or less at a constant temperature, equivalent to the energy scale of the attraction. The glassy phase seems to extend to very low densities. It has been shown with an argument based on the number of effective bonds, that the very low part of the glass curve is not so reliable [26], but experimentally colloidal systems have often been found in a low-density gel state [27].

We now turn to examine the case of the Yukawa fluid. We show here results for $b = 30, 60$ and 100 . The phase diagram for these cases is presented in figure 3. For $b = 30$ the shape of the glass transition is at first sight similar to the case $\epsilon = 0.09$ for SWS in the high-density region, but does in fact show a slight re-entrant behaviour on very close inspection. For $T \rightarrow \infty$ the MCT hard-sphere limit is correctly recovered. Also, the glass line does not seem to extend to very low density. The narrower cases, i.e. $b = 60$ and 100 , show a more evident analogy with the case $\epsilon = 0.03$. In these cases the lines go to low densities and the re-entrant behaviour starts to be present.

Given that the re-entrant behaviour is present in the Yukawa case the question about the presence of the glass–glass transition remains open. We here provide a small argument in favour of the presence of this transition, even for a Yukawa potential, based on preliminary rheological calculations. It is possible to show that the low-frequency shear modulus $G' = G'(\omega \rightarrow 0)$ can be evaluated by [12]

$$G'(\phi, T) = \frac{d^3}{60\pi^2} \int_0^\infty dk k^4 \left(\frac{d \ln S_k}{dk} f_k \right)^2 \quad (20)$$

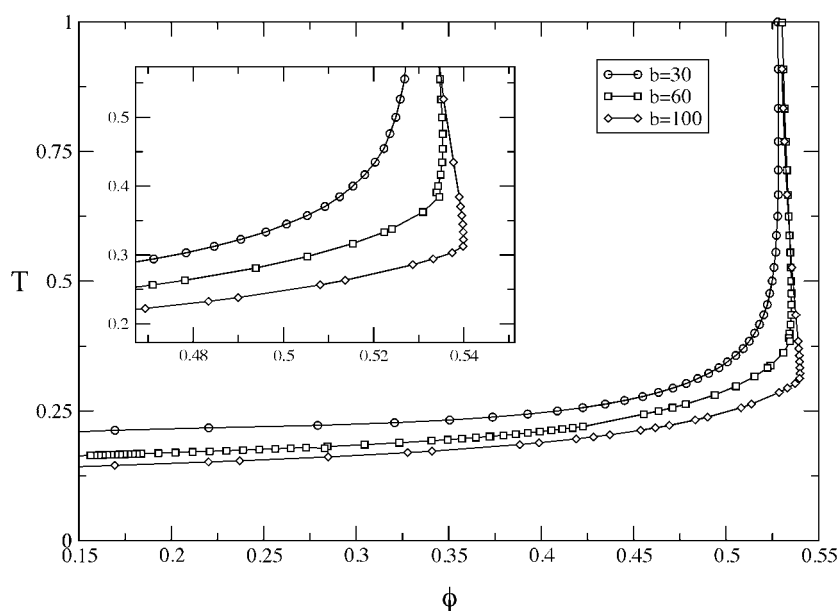


Figure 3. Phase diagram for the Yukawa fluid for screening parameter $b = 30$, $b = 60$ and $b = 100$. In the inset a magnification of the re-entrant part of the lines is shown.

where G' is in units of $k_B T/d^3$. It has been shown that when a glass–glass transition is encountered the value G' presents a sharp transition, being the response to mechanical shear different for the two types of glass [26]. For this purpose, we have evaluated this quantity as a function of the temperature at fixed density for $b = 80.0$. We expect that, for such values of the screening parameter, the system shows the transition we are looking for. In figure 4 we show the behaviour of G' for $\phi = 0.53763$ as a function of the temperature. It is possible to note that the shear modulus present two discontinuities. For $T \simeq 0.333$ the shear becomes suddenly zero and this is the indication that a liquid–glass transition has happened. At a lower temperature, i.e. $T \simeq 0.327$ the discontinuity is between two states of finite shear modulus. The latter case is the clear evidence of a transition between two different glasses. Following this route we have been able to find a few points of the transition and they are represented, together with the liquid–glass line, in figure 5. Of course these points represent just an estimate of the glass–glass transition, and a careful study of the eigenvalues in this region must follow to clearly support this argument. However, it seems likely that, upon further investigation, the presence of the glass–glass transition will be confirmed. Thus, if one accepts this argument, it is interesting to note that the situation here is somewhat different from the SWS case. Indeed, in this case the glass–glass transition line will lie below the liquid region. In other words the liquid phase will be contained in a repulsive glass area. The low-temperature part of this repulsive domain will eventually become an attractive glass. A detailed study of the singularities is currently in progress.

5. Conclusion

In this paper we have discussed the ideal glass transition for two models of attractive colloidal systems, with particular attention being dedicated to the behaviour of the ‘phase diagram’ upon varying the range of the attractions. We have reviewed some of the results for the square-

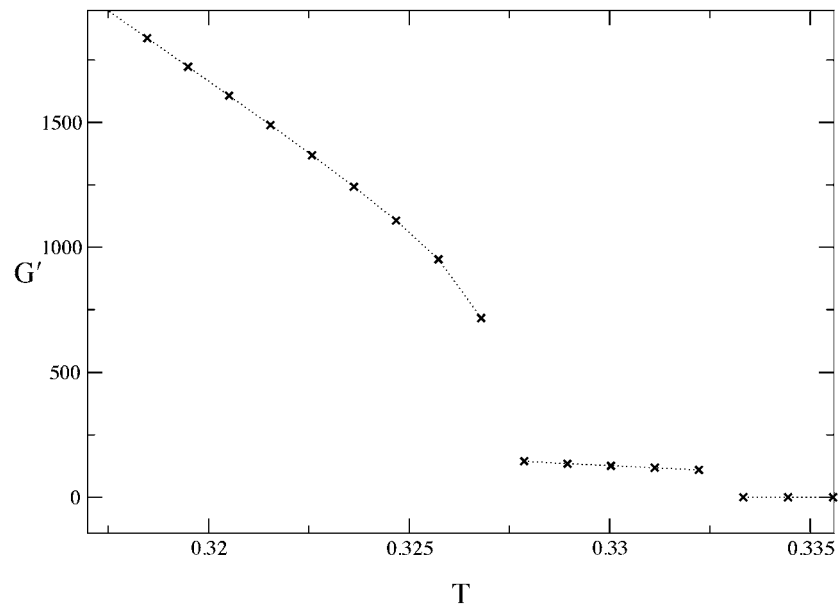


Figure 4. Shear modulus G' at $\phi = 0.53763$ as a function of the temperature in the Yukawa fluid for $b = 80.0$.

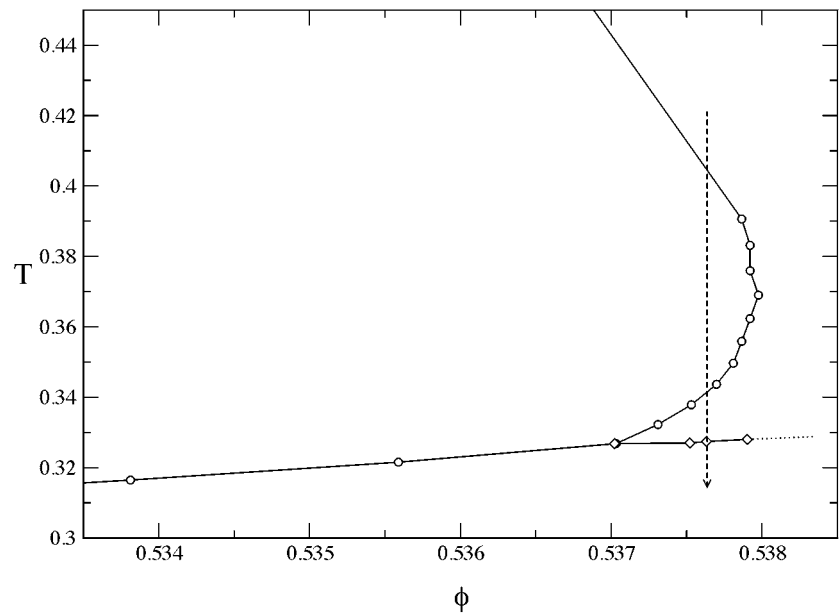


Figure 5. Points of glass–glass transition line estimated from the calculation of the shear modulus. The arrow indicates the direction where G' was evaluated in figure 4.

well potential already reported in [13], and we have also presented some new results for a more realistic and quantitatively accurate model, i.e. Yukawa fluid solved with SCOZA. The comparison of the two models suggests that the main features of the glass line for narrow attractive wells are not dependent on the particular choice of the potential model. In particular,

for a Yukawa system, a re-entrant behaviour of the glass line is found, and some preliminary evidence, based on the study of the shear modulus, seems also to indicate the presence of a glass–glass transition.

Indeed efforts have been also spent in extending the present approach. In particular a new direction has been followed recently in order to overcome some problems of MCT at a more fundamental level. Indeed MCT is an idealized theory and it provides good results only approaching the glass transition since it neglects hopping and aging phenomena. Indeed hopping can be safely ignored in colloidal systems but aging seems to be quite important. In this direction extension of the MCT in order to include aging has been the subject of some recent work [28, 29] but it is too early for quantitative results.

A question to be addressed in the future will be the behaviour of the equilibrium phase diagram of the system with respect to the glass transition. Indeed, one of the advantages of using the SCOZA approach is that it gives a good and consistent account of the thermodynamics. It will be then interesting to study the interplay of critical fluctuation and kinetic arrest. This question has recently started to be addressed [30].

Acknowledgments

We thank D Pini and Professor G Stell for useful discussion on the SCOZA theory. The work in Rome is supported by PRIN-2000-MURST and PRA-HOP-INFM, and the work both in Rome and in Dublin is supported by COST P1.

References

- [1] Pusey P N 1991 *Liquids, Freezing and Glass Transition* ed J-P Hansen, D Levesque and J Zinn-Justin (Amsterdam: North-Holland) p 763
- [2] van Meegen W and Underwood S M 1993 *Phys. Rev. Lett.* **70** 2766
van Meegen W and Underwood S M 1994 *Phys. Rev. E* **49** 4206
- [3] Götze W 1991 *Liquids, Freezing and Glass Transition* ed J-P Hansen, D Levesque and J Zinn-Justin (Amsterdam: North-Holland) p 287
- [4] Götze W 1999 *J. Phys.: Condens. Matter* **11** A1
- [5] Grant M C and Russel W B 1993 *Phys. Rev. E* **47** 2606
- [6] Verduin H and Dhont J K G 1995 *J. Colloid Interface Sci.* **172** 425
- [7] Meller A, Gisler T, Weitz D A and Stavans J 1999 *Langmuir* **15** 1918
- [8] Mallamace F, Gambadauro P, Micali N, Tartaglia P, Liao C and Chen S H 2000 *Phys. Rev. Lett.* **84** 5431
- [9] Fabbian L, Goetze W, Sciortino F, Tartaglia P and Thiery F 1999 *Phys. Rev. E* **59** R1347
- [10] Stell G 1991 *J. Stat. Phys.* **63** 1203
- [11] Foffi G, Zaccarelli E, Sciortino F, Tartaglia P and Dawson K A 2000 *J. Stat. Phys.* **100** 363
- [12] Bergenholtz J and Fuchs M 1999 *Phys. Rev. E* **59** 5706
- [13] Dawson K, Foffi G, Fuchs M, Götze W, Sciortino F, Sperl M, Tartaglia P, Voigtmann Th and Zaccarelli E 2000 *Phys. Rev. E* **63** 1140
- [14] Bolhuis P, Hagen M and Frenkel D 1994 *Phys. Rev. E* **50** 4880
- [15] Dijkstra M, Brader J M and Evans R 1999 *J. Phys.: Condens. Matter* **11** 10 079
- [16] Caccamo C, Pellicane G, Costa D, Pini D and Stell G 1999 *Phys. Rev. E* **60** 5533
- [17] Pini D, Stell G and Wilding N B 2001 *J. Chem. Phys.* **115** 2702
- [18] Piazza R 2000 *Curr. Opin. Colloid Interface Sci.* **5** 38
- [19] Hansen J P and McDonald I R 1986 *Theory of Simple Liquids* (London: Academic)
- [20] Carnahan N F and Sterling K E 1969 *J. Chem. Phys.* **51** 635
- [21] Pini D, Stell G and Wilding N B 1998 *Mol. Phys.* **95** 483
- [22] Baxter R J 1968 *Aust. J. Phys.* **21** 563
Baxter R J 1968 *J. Chem. Phys.* **49** 2770
- [23] Zaccarelli E, Foffi G, Sciortino F, Tartaglia P and Dawson K A 2001 *Europhys. Lett.* **55** 139

- Zaccarelli E, Foffi G, De Gregorio P, Sciortino F, Tartaglia P and Dawson K A *J. Phys.: Condens. Matter* submitted
- [24] Bengtzelius U, Götze W and Sjölander A 1984 *J. Physique C* **17** 5915
- [25] Arnol'd V I 1992 *Catastrophe Theory* (Berlin: Springer)
- [26] Zaccarelli E, Foffi G, Tartaglia P, Sciortino F and Dawson K A 2001 *Phys. Rev. E* **63** 031501
- [27] Krall A H and Weitz D A 1998 *Phys. Rev. Lett.* **80** 778
- [28] De Gregorio P, Sciortino F, Tartaglia P, Zaccarelli E and Dawson K A 2001 *Physica A* (cond-mat/0111018)
- [29] Latz A 2000 *J. Phys.: Condens. Matter* **12** 6353 (cond-mat/0106086)
- [30] Foffi G, McCullagh G, Zaccarelli E, Sciortino F, Tartaglia P, Dawson K A and Pini D *Phys. Rev. E* accepted (cond-mat/0111221)